PNNL-23935

Prepared for the
U.S. Department of Energy
Under Contract DE-AC05-76RL01830

FY14 Progress Report for PL12-LaserSPec SIMS-PD08:

Laser Photoionization of Sputtered Neutral atoms in PNNL SIMS and Applications in Nuclear Materials and Environmental Analyses

DG Willingham
BE Naes
AJ Fahey
SE Thompson
PM: JM Cloutier

December 2014

DISCLAIMER

PACIFIC NORTHWEST NATIONAL LABORATORY
operated by
BATTELLE
for the
UNITED STATES DEPARTMENT OF ENERGY
under Contract DE-AC05-76RL01830

Printed in the United States of America

Available to DOE and DOE contractors from the Office of Scientific and Technical Information,
P.O. Box 62, Oak Ridge, TN 37831-0062
www.osti.gov
ph: (865) 576-8401
fax: (865) 576-5728
email: reports@osti.gov

Available to the public from the National Technical Information Service
5301 Shawnee Rd., Alexandria, VA 22312
ph: (800) 553-NTIS (6847)
or (703) 605-6000
email: info@ntis.gov
Online ordering: http://www.ntis.gov

PNNL- 23935

FY14 Progress Report:

Laser Photoionization of Sputtered Neutral atoms in PNNL SIMS and Applications in Nuclear Materials and Environmental Analyses

DG Willingham
BE Naes
AJ Fahey
SE Thompson
PM: JM Cloutier

Pacific Northwest National Laboratory
P.O. Box 999
Richland, WA 99352

Prepared for the U.S. Department of Energy
under Contract DE-AC05-76RL01830

Pacific Northwest National Laboratory
Richland, Washington 99352

Contents

Figures and Tables

Overview:

A continuous wave (CW) Ar ion laser producing photons at 244 nm (doubled from the fundamental wavelength at 488nm) was used to ionize neutrals sputtered from representative lanthanide (neodymium oxide, Nd_2O_3) and actinide (uranium oxide, U_3O_8) containing materials in the modified Cameca ims-4f at PNNL. Three measurement scenarios (1) ion beam sputtering of the surface only, (2) orthogonal passage of the laser beam approximately 100 μm above the surface only and (3) both ion beam sputtering of the surface and orthogonal passage of the laser beam above the surface were interrogated. The results are indicative of (1) SIMS signal only (traditional analysis method), (2) no signal (laser ablation was not observed) and (3) ionization enhancement over SIMS signal (laser postionization). The magnitude of the ionization enhancement was shown to be heavily dependent on ionization potentials (IPs) of the target analyte. I.E. elemental Nd^+ ion signals from the Nd_2O_3 standard increased >100 times over the comparable SIMS signal, whereas, elemental U^+ ion signals from the U_3O_8 standard were not observed to increase. In contrast to the elemental U^+ ion signals, the UO^+ (IP of 5.6 eV) and UO_2^+ (IP of 5.4 eV) ion signals were shown to increase >5 times and >10 times the comparable SIMS signal respectively. These data support the hypothesis that as the IP of the target analyte increases (Nd at 5.532 eV to U at 6.19 eV), it becomes increasingly more difficult to photoionize the target with the 244 nm output of the Ar ion laser. These results support the hypothesis that increased ionization of actinides (U and Pu) sputtered from solid samples requires photoioniation with photons that contain >1eV more energy per photon than the 244 nm (5.08 eV) output from the Ar ion laser.

Introduction:

Lasers have a long an well documented history of increasing the ionization efficiency of mass spectrometry methods [1,2]. In particular, the implementation of laser postionization for neutrals sputtered from surfaces by high energy ion beams has found utility in analytical methods such as resonance ionization mass spectrometry (RIMS). Because of the wide variety and applicability of pulsed laser systems, much of the research in the literature has focused on time-of-flight (ToF) mass spectrometers where the timing dynamics of the laser system can be integrated effectively into the timing dynamics of the mass spectrometer [3-8]. The major disadvantage of pulsed laser postionization experiments is that they have, by their nature, a very low duty cycle. A ToF mass spectrometer, has a wait time that includes the transit time of all ions through the mass spectrometer to the detector before the next pulse of ions can be intitiated. Short primary ion pulses (50-100 ns) are normally implemented to achieve reasonably high mass resolution. While many high-intensity lasers have short pulse lengths (fs to ns), the ion transit times through a ToF mass spectrometer is typically >100 μs. This results in a duty cycle of approximately 1:10,000. This low duty cycle is redcued further by the fact that most high-power lasers have maximum repetition rates <5 kHz. The duty cycle limitations of pulsed mass spectrometers limits the total number of ions from a sample detectable in a reasonable about of time. Since high precision isotope ratio measurements rely heavily on the ability to detect the maximum number of ions from a

given sample, this becomes a challenge for samples where the concentration of the element of interest is low or the isotope of interest is a minor isotope or both. In a best-case scenario for U of near-natural composition, if only counting-statistical uncertainties are considered, measurements of U isotopes for which a modest precision of 1% is desired of the ^{234}U abundance require detection of 10,000 ions of ^{234}U. This implies that 10^6 ion counts of ^{235}U and 2×10^8 ion counts of ^{238}U would be required. If the detection system and counter operate at the gigahertz level with a small and well-known dead time (so that 10 ^{238}U ion counts can be detected during a single laser pulse (10 ns), then a single measurement of uranium isotopes yielding a 1% uncertainly in ^{234}U requires ~3 hours. This makes characterizing populations of 10 or 20 individual aliquots prohibitively long to measure. Therefore, pulse mass spectrometry methods often suffer from modest precision measurements or require analylsis times that are prohibitively long [9]. Traditional SIMS measurments have addressed this challenge by increasing the duty cycle of the mass spectrometry method by implementing dynamic SIMS instruments (the mainstain of SIMS isotope ratio measurements). Dynamic SIMS has been proven to provide high precision isotope measurements for large sample sets in a relatively short amount of time [10-14]. As a result, an appropriate laser postionization source must also be dynamic or CW. Unfortunately, this limits the available lasers that can be applied to this dynamic laser postionization methodology.

In order to understand the ionization efficiency of a given photon to ionize a give atom, we must investigation photoionization probability. Conceptually the most simple photoionization method is that of non-resonant single-photon ionization (SPI). SPI involves a photoionization scheme in which one photon is sufficient to overcome the IP of a sputtered neutral analyte of interest. Typically, SPI is achieved with ultraviolet (UV) or vacuum ultraviolet (VUV) lasers due to the fact that the ionization potential values for most atoms are in the range of 5-15 eV. A closer look at the photoionization scheme of SPI reveals that the electronic transition resulting from the absorption of a single photon may be described by a conventional photoionization cross-section σ_i. This cross-section is dependent on the ionized atom as well as the spectral characteristics of the ionizing laser (wavelength, spectral line width, etc.). In general, the electron transition will be non-resonant and for atomic species, the resulting cross-section will fall in the range of 10^{-19} to 10^{-17}cm^2. The non-resonant SPI probability can be expressed analytically in equation 1.

$$P_i = 1 - exp(\sigma_i \cdot I_L \cdot t_i) \qquad \text{Eq. 1}$$

The SPI probability (P_i) depends on photon flux density I_L, the photoionization cross-section σ_i, and the effective interaction time t_i that the neutral atom has with the photon. Based on Eq. 1, it is clear that the best-case laser postionization scenario is to use a CW laser with a photon energy that is greater than the IP of the element of interest. Only considering the actinides, a photon energy of at least ~6 eV per photon is required for non-resonant SPI. Assuming a photoionization cross-section of 10^{-17} to 10^{-16} cm^2 (again, best-case), a power density of ~10^8 W/cm^2 would be required in the VUV (>6 eV).

Unfortunately, the CW Ar ion laser explored in this research is not the best-case. Balancing tradeoffs between power, wavelength and duty cycle, the best possible option is to run the CW Ar ion laser at 244 nm where approximately 500 mW of average power can reproducibly be obtained. The major drawback at this wavelength is that the energy per photon at 244 nm corresponds to 5.08 eV. This is >1eV lower than the IP of most of the actinides of interest. When the energy per photon is below the IP of the element of interest, photoionization is more likely to proceed via a non-resonant multiphoton ionization (MPI) mechanism. The non-resonant MPI probability can be expressed analytically in Eq. 2.

$$P_i = 1 - exp\left(\sigma_i^{(n)} \cdot I_L^{(n)} \cdot t_i\right) \qquad \text{Eq. 2}$$

The MPI probability (P_i) depends on all of the factors that the SPI probability does, but is modified by the number of photons needed for the required transition (n). What may not be immediately obvious is that a significant ionization efficiency penalty is paid by transitioning from SPI to MPI. If MPI plays a significant role in the laser postionization mechanism, power densities exceeding 10^{10} W/cm^2 are required for effective photoionization of sputtered neutrals (these densities can only be reached by pulsed lasers) [15].

The previous analytical expressions are applicable for ground-state energy equilibratied atoms interacting with photons. However, these equations do not account for non-equilibrium conditions. This is advantageous for sputtered neutrals where a number of studies have shown that non-equilibrium conditions are prevalent [16,17]. Our hypothesis is that when atoms are liberated from surfaces (e.g., metals or oxides), a few electronvolts of energy is required; therefore, it is likely that the electronic states of the liberated atom are elevated (increase internal energy) and quickly move toward an equilibrium with its translational energy (relax to the ground-state). As a result, many reports have suggested that sputtered atoms exhibit increased interal energy distributions residing in relatively long-lived excited states [18-20]. It is unclear, however, (1) whether a significant fraction of the sputtered neutrals may exist in these excited states, (2) exactly how much internal energy they possess and (3) for how long they remain excited before returning to the ground-state. It is our hope that there is a significant fraction of excited state sputtered neutrals and that they exist long enough to photoionize them with the CW Ar ion laser at 244 nm by non-resonant SPI.

The goals of this study are fourfold (1) determine whether the ionization efficiency of lanthanides and actinides can be increased using CW photoionization at 244 nm, (2) identify whether the ionization efficiency is highly dependent on the IP of the element of interest, (3) measure the most probable velocity of the sputtered neutrals as compared to the secondary ions and (4) measure the isotope ratios of the elements of interest. These goals aim to not only observe ionization enhancements, but also to confirm that these enhancements are suitable for high precision isotope ratio measurements.

Experimental

The mass spectrometer used for this study is a modified CAMECA ims-4f secondary ion mass spectrometer. The primary beam column has two ion sources selectable by a magnetic mass filter and three lenses along with a series of deflectors and stigmators to direct and shape the beam. For this study an O^- beam of -12.5keV energy was extracted from the duoplasmatron source. The secondary column is run at +6 keV to accept positive ions with an imaged field of ~150 μm. Thus, the impact energy of O^- is 18.5 keV. This instrument is a stigmatic ion microscope and is described in detail elsewhere[16]. A CW argon ion laser capable of producing ~500 mW of average power at 244 nm was coupled to the ims-4f mass spectrometer via a specific designed optics system that allowed the 244 nm light to be focused ~100 μm above the sample surface. Because the CAMECA ims-4f was not designed for laser postionization, a complete laser alignment procedure involving (1) measuring the beam profile entering the vacuum, at the focus and exiting the vacuum, (2) independent, single axis manipulation of the laser beam in the the X,Y and Z directions and (3) careful centering on entrance and exit aperutures could not be finalized. Despite these challenges and due to a number of permissible modifications that were made to the CAMECA ims-4f design, an initial alignment procedure was devised allowing preliminary data to be obtained.

Results and Discussion

Preliminary laser postionization validation methods encompassed a fourfold approach focused on (1) on-off-on temporal experiments, (2) comparable stability of isotopic ratio studies, (3) determination of the most probably ejection velocities for both ions and neutrals and (4) a feasibility of particle analysis assessment.

On-off-on Experments:

In these experiments, three different physical states are probed as a function of signal evolution in time. The first is indicative of laser postionization signal where both the primary ion beam impinges on the sample surface and the photoionization laser is positioned orthogonally above the sample surface. The ion signal collected in this mode is dependent both on the primary ion beam and the positionization laser. The second represents the traditional SIMS analysis were the primary ion beam impinges on the sample surface, but the photoionization laser is blocked with a mechanical shutter. The ion signal collected in this mode is dependent only on the primary ion beam and is characterized simply by the secondary ion yield. Finally, the laser mode involved having the photoionization laser in position above the sample surface, but turning off the primary ion beam. The ion signal, if any, collected in this mode is dependent only on the positionization laser and is studied primarily to observe any inadvetant laser ablation that may be taking place.

Two primary samples were analysed in this on-off-on modality; CRM-112a particles (U_3O_8) on a silicon substrate shown in Fig. 1 and bulk neodymium oxide (Nd_2O_3) power. The CRM-112a particle analysis was truncated and, therefore, only showed observations of laser postionization signal (the first mode) and SIMS (the second mode). These observations were toggled by opening and closing a mechanical shutter that either allowed or blocked the postionization laser to enter the mass spectrometer. Ion yield enhancements were shown for the UO_2^+ positionization signal derived from the U_3O_8 particles on the order of 10 times greater than the traditional SIMS signals. This enhancement was observed to persist over a period of 15 minutes. The ion signal was shown to decrease slightly with time; likely due to eventual consumption of the U_3O_8 particles. The analysis shown in Fig. 1 suffers from two main experimental flaws, (1) the third mode of the on-off-on methodology was not measured and, therefore, direct interaction of the positionization laser with the U_3O_8 particles cannot be ultimately ruled-out and (2) the U_3O_8 particles analyzed did not provide a stable signal over a long enough time period to rule-out the possibility of charging or charge-compensation behavior.

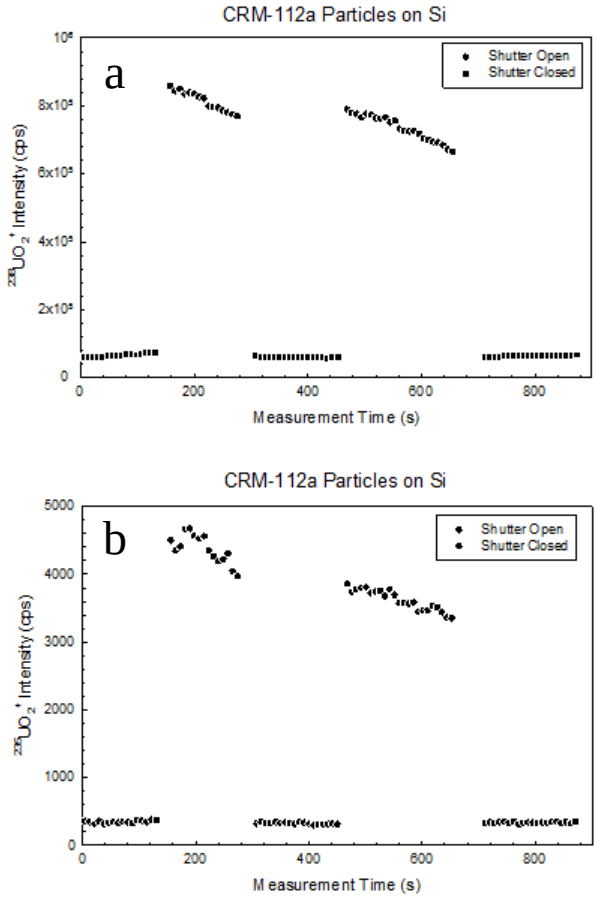

Fig. 1: On-off-on temporal plots of the $^{238}UO_2^+$ (a) and the $^{235}UO_2^+$ (b) ion signal response of CRM-112a U_3O_8 particles on a Si substrate.

In order to build on the first experiment, bulk Nd_2O_3 power was studied. The analysis of bulk Nd_2O_3 provides three distinct advantages over the CRM-112a particle anlaysis; (1) this analysis included the laser only mode eliminating the possibility of ion signal from inadvertent laser ablation, (2) analysis of the bulk provided a stable ion signal over a time period of 90 minutes compared the the previous 15 minute experiment and (3) the choice of Nd_2O_3 provided neutrals with much lower I.P.s (~5.5 eV) resulting in higher photoionization probabilities and thus higher postionization yields. The results from the on-off-on technique for Nd_2O_3 are shown in Fig. 2. Unlike the U_3O_8 experiment that did not yield ion enhancement for the elemental U^+ ions, the lower I.P.s of Nd^+ (red) and its associated oxides (NdO^+, black and NdO_2^+, green) yielded observed enhancements for both elemental and oxide ions. Additionally, these ion enhancements were orders of magnitude larger than for U_3O_8 particles indicating that the photon energy of the Ar ion laser is not sufficiently high enough to ionize U neutrals with a high photoionization probability; which is why no elemental U^+ ion enhancements were observed.

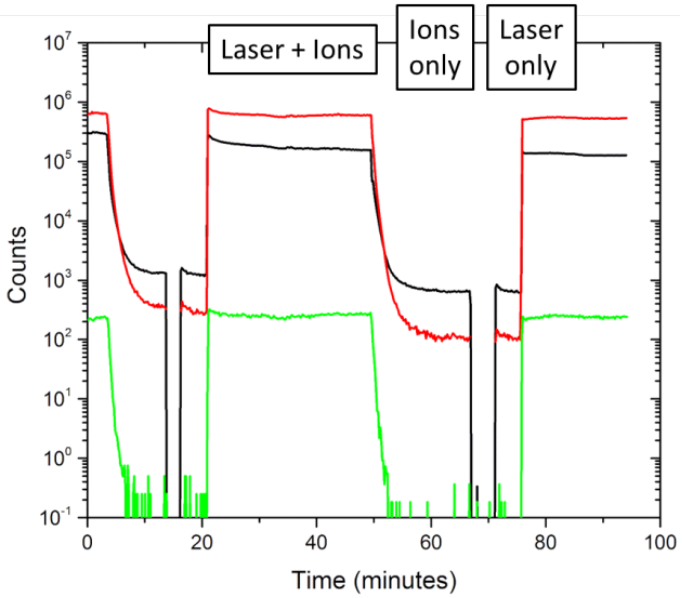

Fig. 2: On-off-on temporal plots of the Nd^+ (red), NdO^+ (black) and NdO_2^+ (green) ion signal response of bulk Nd_2O_3 powder pressed into In foil. Three experimental states are shown (1) laser + primary ions, (2) primary ions only and (3) laser only.

Isotope Ratio Studies:

To this point, the focus of this work has been solely on enhancements in ion yields. The following work will be used to validate whether or not the observed ion enhancements are useful; meaning they can actually be used to supplement the standard SIMS signals. The first and probably most important aspect of useful ions signals is

whether or not they can be used for high accuracy and precision isotope ratios. The first attempt at validating laser postionization isotope ratios can be observed in Fig. 3. Here, the ratio of $^{235}UO_2^+/^{238}UO_2^+$ for both SIMS and laser positionization signals evolved from CRM-122a particles on a Si substrate are compared. Again, it must be noted that UO_2^+ ion signals were used in the absence of elemental U^+ ion enhancements and that traditional SIMS anlaysis of U_3O_8 focuses soley on elemental U^+ ion signals. Fig. 3 shows that the $^{235}UO_2^+/^{238}UO_2^+$ ratio for SIMS signal (laser blocked) changed very little maintining an average value of ~0.00525±0.00025; the NIST certified value of the $^{235}U/^{238}U$ ratio is reported as 0.0072543. This indicates that there is significant mass fractionation between the elemental U^+ isotopes and the UO_2^+ isotopes. Additionally, while the laser postionization ions have a higher precision due to the observed ion enhancements, the accuracy of the $^{235}UO_2^+/^{238}UO_2^+$ ratio varies from ~0.0055 to ~0.0050 (these two numbers are statistically different considering the enhance precision of the measurement). This isotope ratio measurement suffers from two main difficulties (1) the measured ratio is significantly different from the certified NIST value and (2) the two laser postionization measurement blocks (at 200 seconds and 550 seconds) are significantly different from each other. This means that although there is enhanced ion signal due to laser positionization, the isotope ratios obtained from these signals is only stable enough from moderately accurate isotopic analysis.

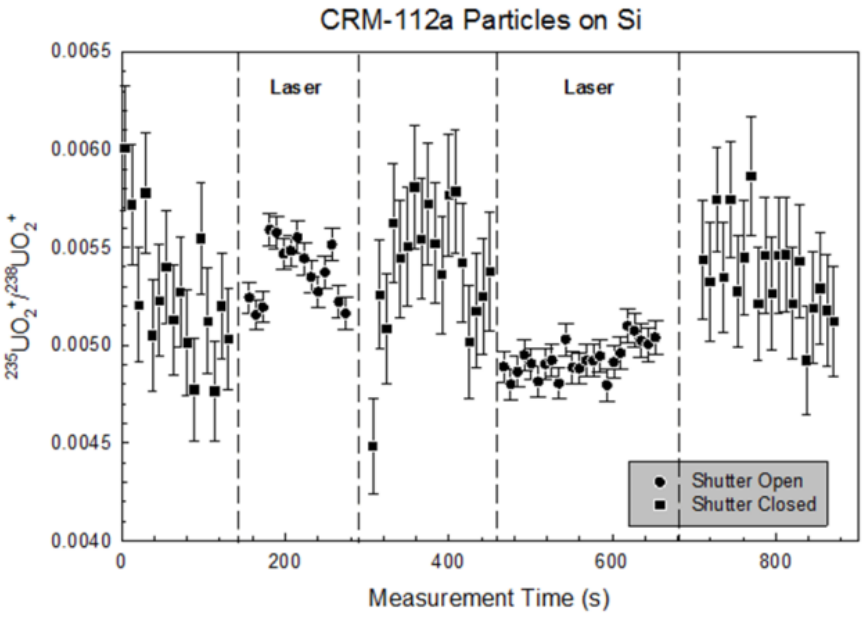

Fig. 3: On-off-on temporal plots of the $^{235}UO_2^+/^{238}UO_2^+$ isotope ratio of CRM-112a U_3O_8 particles on a Si substrate.

In order to build on this first isotope ratio experiment, bulk Nd_2O_3 power was again studied. The analysis of bulk Nd_2O_3 provides two distinct advantages over the

CRM-112a particle anlaysis; (1) elemental Nd^+ ion signals were observed with both SIMS and laser positionization measurments and (2) Nd has several naturally occurring isotopes and, therefore, provides a number of comparable points for validation with certified values. It must be noted that the isotopic composition of the Nd_2O_3 powder was believed to be that of naturally occurring Nd. Fig. 4 illustrates the isotope ratio data taken for Nd_2O_3 for both SIMS (red) and laser positionization (black). Instead of simply looking at the isotope ratio as a function of time, an average value with uncertainties (top and bottom capped bars) was taken for the entire analysis time spanning over an hour of interleaved SIMS and laser postionization measurements. These isotope ratios were compared with the natural distribution of Nd isotopes using ^{144}Nd as a reference and were reported in Fig. 4 as delta values. Delta values are more commonly used than the straight isotope ratios because of their ability to highlight small differences in mass fractionation between isotopes. Fig. 4 shows that, for elemental Nd isotopes, the laser postionization isotope ratios have increased precision of the comparable SIMS data without sacrificing accuracy. Unlike the CRM-112a particle data, the laser positionization ion enhancement is useful for high precision and accuracy isotope ratio measurements. Again, the Nd_2O_3 bulk data showed high precision and accuracy isotope ratio measurements with ion enhancements on the order of several orders of magnitude.

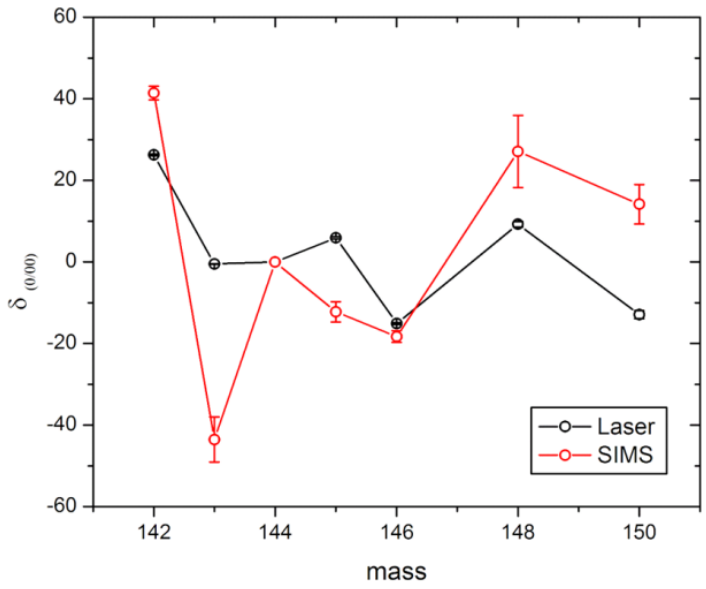

Fig. 4: Deviation of each Nd isotope (^{142}Nd-^{150}Nd) from accepted literature values using ^{144}Nd as the reference isotope for both laser postionization (black) and SIMS (red).

Energy/Velocity Analysis:

Another very important consideration for mass spectrometry is the extraction energy and dependently the velocity of ions into the mass spectrometer. Because the

sputtered neutrals in a laser positionization experiment are being ionized above the sample surface, they are extracted at a slightly different energy and velocity than the direct secondary ions. If the energy difference is too great, the laser positionization ions will not be effectively extracted into the mass spectrometer and, therefore, will be lost. In order to validate that the extraction energy/velocity distribution of the laser postionization ions is within the tolerances of the mass spectrometer, the ion signal for both SIMS and laser postionization was monitored as a function of the sample high voltage. By tuning the mass spectrometer to accept only a very small range of energies, the most probable ejection energy/velocity can be determined. This data for analysis Nd^+ ion and NdO^+ ion from bulk Nd_2O_3 can be found in Fig. 5. for both SIMS (red) and laser postionization (black) signals. As expected, the peak energy/velocity is slightly different between the SIMS and laser postionization signals; however, each is within the tolerances for acceptance into the mass spectrometer. Interestingly, the NdO^+ ion signals show a large separation in peak energy/velocity than the correlatary Nd^+ ion signals. This observation, in itself, is interesting and is possibley characteristic of Nd^+ ion signals resulting from fragmentation of NdO and NdO_2 neutrals. This lends support to the hypothesis that elemental signals with higher I.P.s can be derived from photoionization of their associated oxides with lower I.P.s. This is likely the reason for obsereved elemental Nd^+ ion signals even though the I.P. of Nd is ~0.5 eV higher than the achievable photon energy at 244 nm.

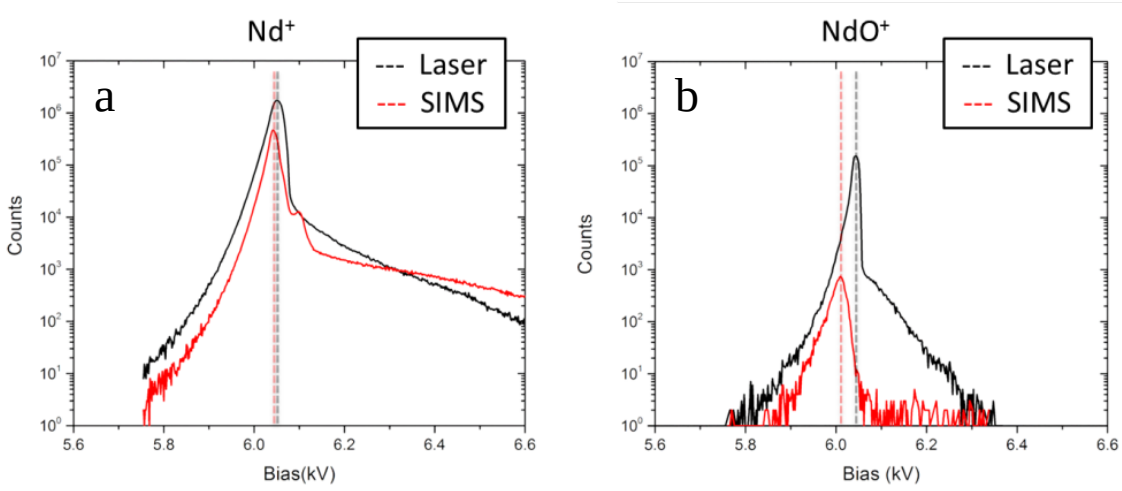

Fig. 5: Nd^+ (a) and NdO^+ (b) ion signal response as a function of extraction voltage for both laser postionization (black) and SIMS (red). Dashed lines indicate the most probable energy/velocity of ejected ions/neutrals.

Particle Analysis:

One of the major analytical areas that would most benefit from enhaced ionization efficiency is that of particle analysis. Particles represent atom limited samples

where it is paramount to obtain as many ion counts as possible before the whole of the sample is exhausted. Fig. 6 illustrates the analysis of CRM-112a particles dispersed on a Si planchette. In the experiment the UO_2^+ signal was analyzed with the laser shutter open (a) and the laser shutter closed (b); similar to the on-off-on experiments described previously. As before, the UO_2^+ ion signal increases under laser positionization conditions several times over traditional SIMS analysis (laser off). Additionally, the particle analysis shows that only particles directly under the focus of the laser experience the full enhancement in ionization. This observation indicates (1) that the laser is, indeed, focused to its minimum achievable spot size and (2) that laser ablation of the surface is not occurring. It is clear from this analysis that enhance ionization of particles is possible with laser positionization.

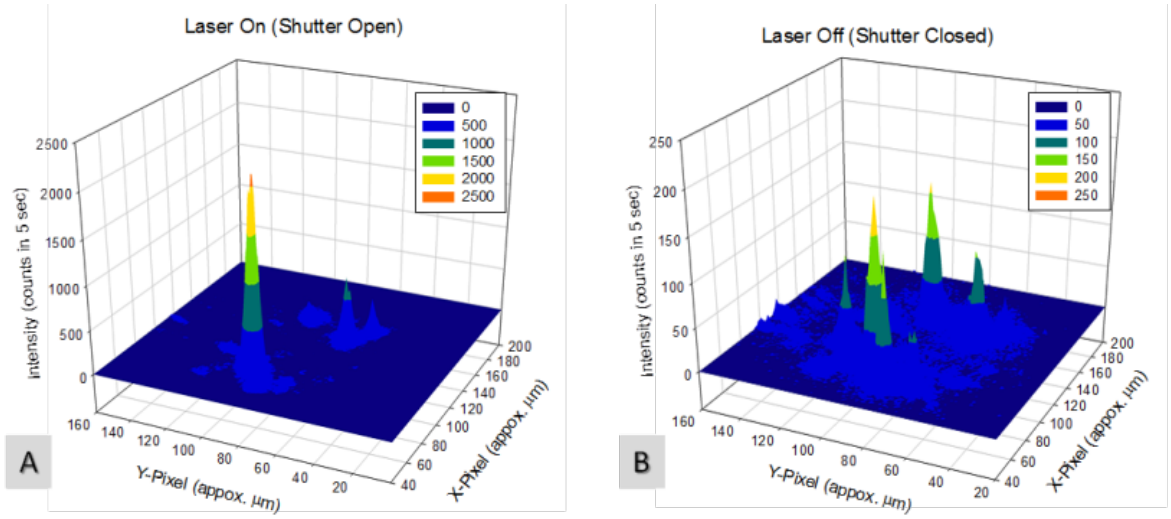

Fig. 6: Particle analysis of CRM-112a U_3O_8 particles on a Si substrate. The intensity plots indicate the UO_2^+ ion signal during laser postionization (a) and SIMS (b).

Conclusion

Preliminary results show that laser postionization can be used to increased the ionization efficiency of dynamic SIMS experiments. The exact magnitude of ionization enhancement is, however, heavily dependent on the IP of the element of interest. This is clearly shown by comparing the ionization response of Nd^+, NdO^+ and $NdO_2^+$with UO_2^+. Unfortuanely, the two orders of magnitude increase in ionization efficiency for actinides was not realized. This is primarily a result of the photon energy of the Ar ion laser being ~1 eV lower than the IP of U and other actinides. The only forseable way to overcome this restriction is to increase the photon energy of the light sources (i.e. move to a lower wavelength). The use of a VUV lamp to produce higher energy photons has been proposed for the FY15 scope.

Acknowledgements

We would like to acknowledge the efforts of Dr. David Gerlach who originally conceived of this work and laid the groundwork for the effort, but passed away before being able to see any of it come to fruition. Also, Dr. Albert Fahey, who is now at the Naval Research Laboratory, for his contribution to the initial direction of this project.

Reference List

[1] Wendt K, Trautmann N (2005) International Journal of Mass Spectrometry 242:161
[2] Wendt K, Trautmann N, Bushaw BA (2000) Nucl Instrum Meth B 172:162
[3] Brummel CL, Willey KF, Vickerman JC, Winograd N (1995) Int J Mass Spectrom 143:257
[4] Willingham D, Brenes DA, Wucher A, Winograd N (2010) J Phys Chem C 114:5391
[5] Willingham D, Kucher A, Winograd N (2009) Chem Phys Lett 468:264
[6] Willingham D, Savina MR, Knight KB, Pellin MJ, Hutcheon ID (2013) J Radioanal Nucl Ch 296:407
[7] Winograd N (1993) Anal Chem 65:A622
[8] Wood M, Zhou Y, Brummel CL, Winograd N (1994) Anal Chem 66:2425
[9] Fahey AJ, Messenger S (2001) International Journal of Mass Spectrometry 208:227
[10] Eiler JM, Graham C, Valley JW (1997) Chem Geol 138:221
[11] Esaka F, Magara M, Suzuki D, Miyamoto Y, Lee CG, Kimura T (2010) Talanta 83:569
[12] Fitzsimons ICW, Harte B, Clark RM (2000) Mineral Mag 64:59
[13] Slodzian G (2004) Appl Surf Sci 231:3
[14] Tamborini G, Phinney D, Bildstein O, Betti M (2002) Anal Chem 74:6098
[15] He C, Becker CH (1996) Curr Opin Solid St M 1:493
[16] Krantzman KD, Kingsbury DB, Garrison BJ (2007) Nucl Instrum Meth B 255:238
[17] Teodoro OMND, Maneira MJP, Moutinho AMC (1994) Vacuum 45:15
[18] Suchanska M (1997) Prog Surf Sci 54:165
[19] Tsong IST, Yusuf NA (1978) Appl Phys Lett 33:999
[20] Williams P, Tsong IST, Tsuji S (1980) Nuclear Instruments & Methods 170:591